An empirical study of an agglomeration network

2007 J. Phys. A: Math. Theor. 40 12365

(http://iopscience.iop.org/1751-8121/40/41/007)

J. Phys. A: Math. Theor. **40** (2007) 12365–12375 doi:10.1088/1751-8113/40/41/007

An empirical study of an agglomeration network

Yichao Zhang[1], **Zhaochun Zhang**[2] **and Jihong Guan**[3]

[1] School of Material Science and Engineering, Shanghai University, 200072, Shanghai, People's Republic of China
[2] School of Material Science and Engineering, Shanghai University, 200072, Shanghai, People's Republic of China
[3] Department of Computer Science and Technology, Tongji University, 4800 Cao'an Road, 201804, Shanghai, People's Republic of China

E-mail: jhguan@mail.tongji.edu.cn

Received 29 January 2007, in final form 5 July 2007
Published 25 September 2007
Online at stacks.iop.org/JPhysA/40/12365

Abstract

Recently, researchers have reported many models mimicking real network evolution growth, among which some are based on network aggregation growth. However, until now, relatively few experiments have been reported. Accordingly, in this paper, photomicrographs of real materials (the agglomeration in the filtrate of slurry formed by a GaP-nanoparticle conglomerate dispersed in water) are analyzed within the framework of complex network theory. By data mapping from photomicrographs we generate undirected networks and as a definition of degree we adopt the number of pixel's nearest neighbors while adjacent pixels define a connection or an edge. We study the topological structure of these networks including degree distribution, clustering coefficient and average path length. In addition, we discuss the self-similarity and synchronizability of the networks. We find that the synchronizability of high-concentration agglomeration is better than that of low-concentration agglomeration; we also find that agglomeration networks possess good self-similar features.

PACS numbers: 05.10.−a, 05.45.Df, 82.35.Np, 89.75.−k

(Some figures in this article are in colour only in the electronic version)

1. Introduction

Since the pioneering work by Watts and Strogatz on small-world networks [1] and Barabási and Albert on scale-free networks [2], complex networks have provided a natural framework to describe a variety of large systems in many disciplines of science and have recently received much attention from scientific communities [3–7]. In the past few years, large numbers of models have been proposed aiming at reproducing statistical properties of real-world networks

[8–17]. Meanwhile, another group of complex network studies aims to investigate certain dynamical problems on network topologies [18–21]. A third group of works studies the empirical evidence collected from real data [22–34]. In these works, a real system can be described by a complex network with nodes (or vertices, or points) representing individuals, organizations, computers, etc, and links among them representing their interactions. Although a large number of empirical researches have been done, complex network theory has not been applied in material sciences as far as we know and we hope to shed some new light on the field by adopting network language.

On the other hand, in material science, the vibrational spectra can give more detailed molecular structural information. Raman spectra have been shown to be well suited for the vibrational investigation of compounds. To the best of our knowledge, most attention has been given to the substrate and many theories have been introduced to explain the intensity enhancement [35, 36]. However, no precise explanations about how complex material structure affects Raman spectrum intensity have been reported. This problem leads us to consider the relation between the topological structure of agglomeration and the aggregating processes in the hope of giving a rational explanation of the relation. Furthermore, because the robustness of a material has a close relation to endurance, conductance and other material properties, to quantify the robustness of a network against intentional or random attack is a crucial subject also for material researchers.

In this paper, we first report an experiment and directly use complex network theory to convert real agglomerations into network models. With the intention of studying the topological properties of the networks, degree distribution, clustering coefficient, correlation between degree and clustering coefficient, average path length, and degree correlation are obtained in this paper. In addition, self-similarity and synchronizability behavior are discussed. Moreover, we discuss the corresponding meanings of these structural parameters from the perspective of material researchers. In a word, this work establishes that the properties of materials can to some extent be reflected by the mapped networks.

2. The experiment

200 mg GaP particles were placed in an Erlenmeyer flask filled with 50 ml deionized water. The resulting slurry was dispersed by agitation for about 24 h and separated by filtration. (The filter membrane was made of synthetic fabric ester; the aperture was 220 nm). A few fragments of the membrane coupled with permeating particles had been gradually associating for four years and turned to agglomerations. In the solution, the structures of these two agglomerations were three-dimensional and mobile; but, for the sake of analysis, they had to be fixed and captured in the form of two-dimensional images. Hence a small portion of the solution was removed from the flask and placed on a glass slide. After evaporation of the water these glass slides were placed under an optical microscope (VHX-100K digital metallography microscope). We chose to study the most integrated agglomerations in low- and high-concentration solutions, respectively. The optical microscope pictures (500 times magnified) are shown in figure 1.

In this paper, two slices of the surfaces of different agglomerations in high- and low-concentration solutions are selected as objects for research. Then, in order to establish our conclusion (regarding synchronizability in section 3.6) we chose to test two close arrayed points (approximately the same number of particles as in the laser spot) in high- and low-concentration agglomerations coupled with different topology structures. The Raman spectra were recorded by a Horiba Jobin Yvon 800 UV Raman spectroscope. The sample was illuminated with the 514 nm line of an Ar laser in a backscattering geometry. To avoid thermal effects, in typical experiments the laser beam power at the sample surface was 15 mW with a light spot diameter

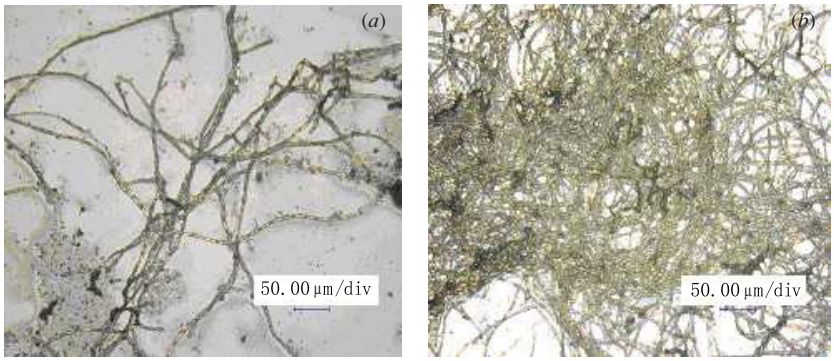

Figure 1. Optical microscope pictures of agglomerations in (*a*) the low-concentration solution and (*b*) the high-concentration solution, respectively.

of about 2 μm. The spectra were measured in the Stokes spectral range between 1800 and 900 cm^{-1}. The scattered photons were detected by a cooled photomultiplier with a spectral resolution of 1 cm^{-1}. It should be pointed out that the scattering intensities of the two different samples were measured with the same apparatus and under identical conditions so that the values of the intensity were comparable.

3. Structural properties

Data mapping from pictures is an interesting and important task in our work. A pixel of uniform color and gray level is defined as a node; in the meantime the pixels around it take the role of neighbors. Then two slices with the same color and gray level are acquired from the pictures: see figure 2. In fact there are slight changes between figures 1(*a*), (*b*) and figures 2(*a*), (*c*). Under the available conditions, we were only able to slice the highest parts with relatively uniform gray levels, while the lower parts of figures 1(*a*), (*b*) were treated as agglomerations on different planes. On the other hand, the dimensions of the pictures were adjusted slightly to fit the needs of analysis. The agglomeration in figure 2(*b*) is made up of 358 pixels and 1107 edges, while that in figure 2(*d*) has 896 pixels and 3208 edges. The resulting networks of pixels are presented in figure 2. The number of nodes in these two networks is equal to the number of pixels they have. In what follows these two networks will be the main research objects of this paper.

3.1. Degree distribution

The degree (or connectivity) k_i of a node i is the number of edges incident with the node, and is defined in terms of the adjacency matrix A as

$$k_i = \sum_{j \epsilon n} a_{ij}, \tag{1}$$

where $n \equiv n_1, n_2, \ldots, n_N$ are the nodes of the graph. The degree distribution $P(k)$ is one of the most important and basic statistical characteristics of a network. By definition, the degree distribution $P(k)$ is the probability that a randomly selected node has exactly k edges.

Unlike the small-world [1] and scale-free networks [2], the degree distribution in our agglomeration networks is variable (see figure 3). These results indicate that the probability at which k pixels link a certain pixel does not follow a 'rich-gets-richer' principle. By contrast,

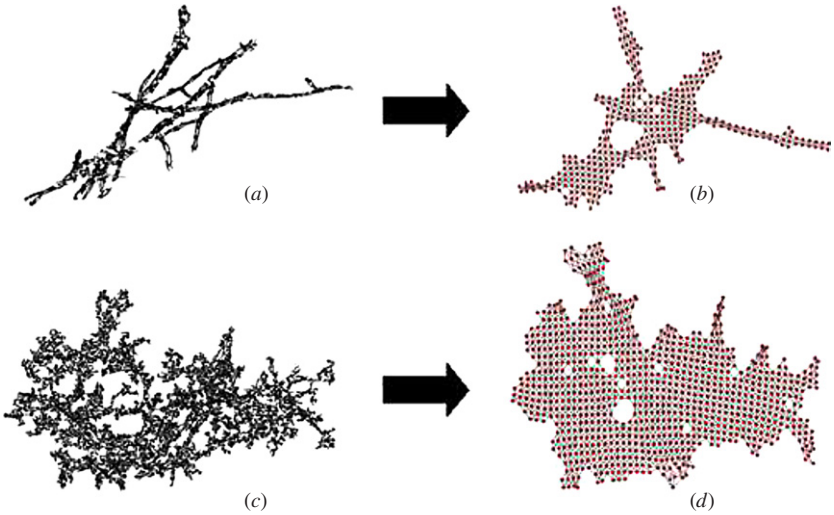

Figure 2. (*a*) A piece of surface slice of figures 1(*a*) and (*b*) its network in the mode of kamada-kawa energy, (*c*) a piece of surface slice of figures 1(*b*) and (*d*) its network in the mode of kamada-kawa energy.

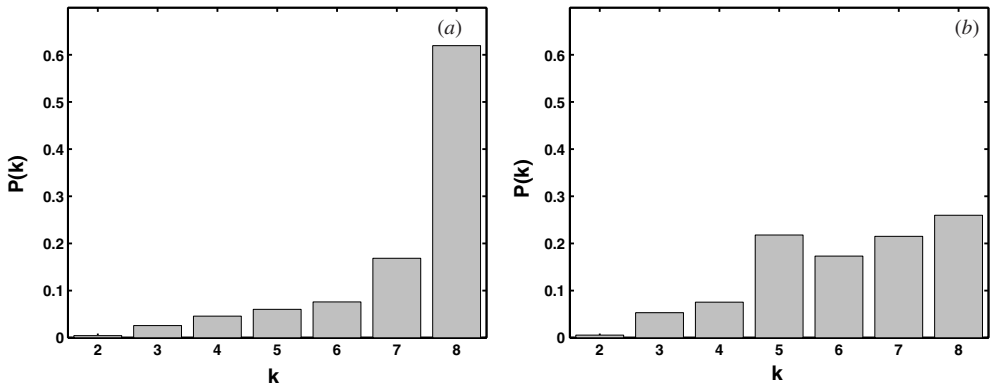

Figure 3. Degree distribution $P(k)$ versus k for (*a*) the high-concentration agglomeration network and (*b*) the low-concentration network.

certain pixels tend to have eight neighbors in the two different agglomeration networks as limited by the Euclidean space.

Under fixed temperature and pressure, for a given quantity of liquid, the surface work $\partial W'$ needed to extend a surface is directly proportional to the surface area change $\mathrm{d}A$. If σ stands for the constant of proportionality, one has

$$\partial W' = -\sigma \mathrm{d}A. \tag{2}$$

If the surface extending process is reversible, $\partial W' = -\mathrm{d}G_{T,p}$, where $G_{T,p}$ is the Gibbs free energy under fixed temperature and pressure. Equation (2) can be also presented as

$$\mathrm{d}G_{T,p} = \sigma \mathrm{d}A, \tag{3}$$

or

$$\sigma = \left(\frac{\partial G}{\partial A}\right)_{T,p}. \tag{4}$$

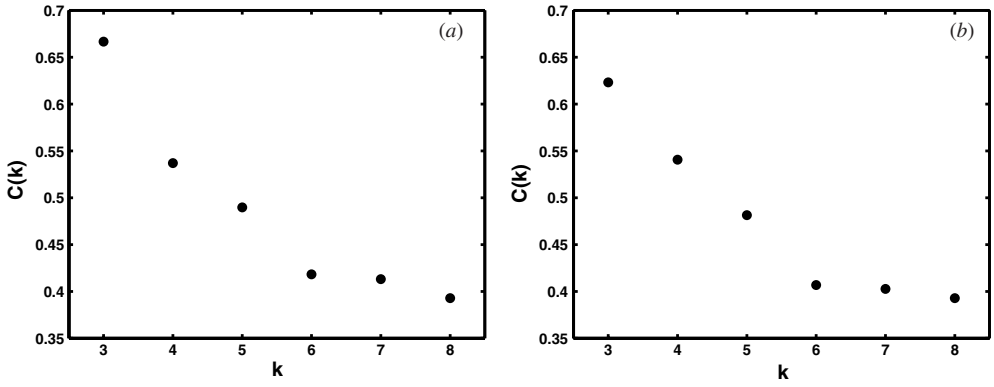

Figure 4. Clustering coefficient $C(k)$ versus the node degree k for (a) the low-concentration agglomeration network (b) the high-concentration network.

For decreasing system energy and on approaching a steady state, agglomerations tend to a more compact state in order to reduce surface area, that is, to reduce the exposed perimeter of whole agglomerates when the number of particles is fixed. Hence, the agglomerations at high concentration have more nodes with a larger degree than those at low concentration.

3.2. Clustering coefficient

The clustering coefficient provides a measure of the level of cohesiveness around any given node. A quantity C_i (the local clustering coefficient of node i) is first introduced, expressing how likely $a_{jm} = 1$ for two neighbors j and m of node i. By definition, the clustering coefficient C_i [4] of node i is the ratio between the number of edges E_i which actually exist among the k_i neighbors of node i and its maximum possible value, $k_i(k_i - 1)/2$, i.e.,

$$C_i = 2E_i/k_i(k_i - 1). \tag{5}$$

The average clustering coefficient $\langle C \rangle$ of the whole network is the average of all individual C_i's,

$$\langle C \rangle = \frac{1}{N} \sum_{i \epsilon n} C_i. \tag{6}$$

Here we compute exactly the clustering coefficient for every node and the average value for the network. Through calculation we find that the average value of C_i is 0.4459 in the low-concentration agglomeration and 0.4118 in the high one. Meanwhile, the relation between C_i and k is shown in figure 4. Low-concentration agglomerations with fewer nodes have a larger clustering coefficients. The result indicates that spatial factors strongly limit the aggregating process.

3.3. Self-similarity

Enlightened by Song and Havlin's seminal work [37, 38], we adopt the maximum-excluded-mass-burning algorithm (MEMB) [39] to estimate the topological fractal dimension of these networks and choose vertices which have the largest degree as hubs. There are three reasons: firstly, there must exist a path inside a box that connects two nodes belonging to this box; secondly, it is by far the easiest to implement; thirdly, the hubs exist in our networks. The boxes contain nodes separated by a distance l_B, which is measured as the length of the shortest

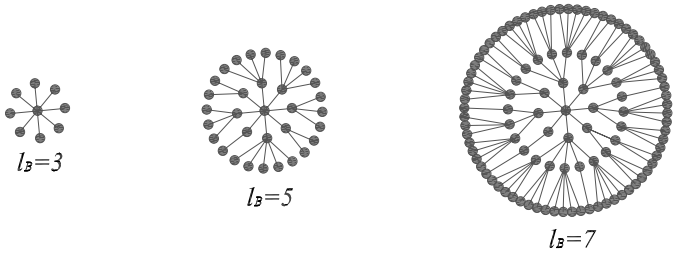

Figure 5. Illustration of boxes of path (or border) lengths $l_B = 3, 5, 7$ for use in the MEMB algorithm.

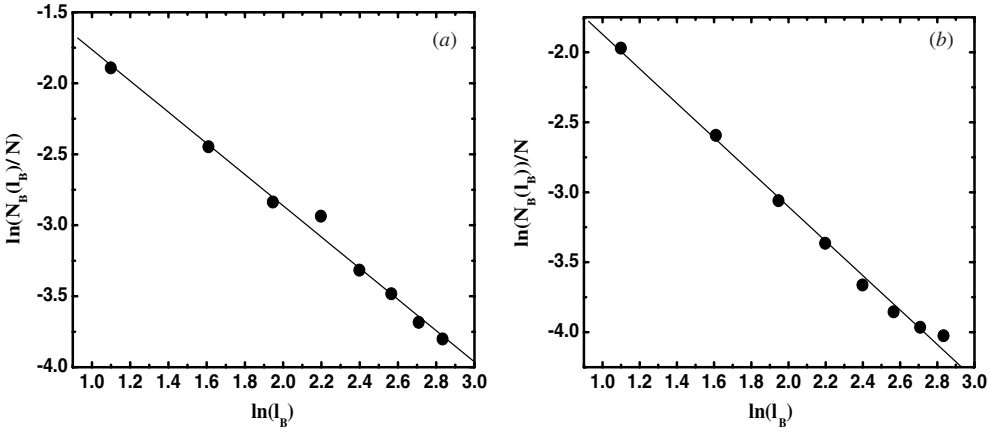

Figure 6. Logarithmic plot of the border length l_B and the number of boxes N_B at (*a*) low concentration, and (*b*) high concentration, respectively.

path between nodes. Each box is subsequently replaced by a node, and the process is repeated until the whole network shrinks to a single node. The relation between l_B and the size of the boxes is shown in figure 5. For each value of the box size l_B, we search for the number of boxes needed to tile the entire network such that each box contains nodes separated by a distance $l < l_B$.

Then, to estimate the topological fractal dimension, d_B, we fit the number of required boxes $N_B(d_B)$ to the expression

$$\frac{N_B(l_B)}{N} \approx l_B^{-d_B}, \tag{7}$$

which we accept as defining d_B. From figure 6, we can obtain the results $d_B = 1.10 \pm 0.04$ for low concentration and $d_B = 1.23 \pm 0.04$ for high concentration. That is to say, self-similarity does exist in the present agglomeration networks. The MEMB algorithm provides a powerful tool for further investigations of network properties, because it enables a renormalization procedure, revealing the topological self-similarity of agglomerations. The self-similarity of one agglomeration is not only a parameter to depict the robustness against intentional or random attack but also a way to differentiate the sort of specimen structure containing the same ingredient. Hence, it provides a new way to describe various material structures.

3.4. Average path length

The shortest paths play an important role in the transport and communication within a network. Suppose one needs to make a call to a friend through the telephone net: the geodesic provides an optimal path, since one would achieve a fast transfer and save system resources. For such a reason, the shortest paths have also played an important role in the characterization of the internal structure of a graph.

The path length of a pair of vertices is defined as the shortest distance (the length of the shortest path) between them, which characterizes the communication delay in the network [40]. A measure of the typical separation between two nodes in the graph is given by the average path length (APL), also known as the characteristic path length, defined as the mean of geodesic lengths over all pairs of nodes,

$$D = \frac{1}{N(N-1)} \sum_{i,j\epsilon n, i\neq j} d_{ij}. \tag{8}$$

We find that the APL in our low-concentration network is 14.0 and 16.6 in the high-concentration network. Although the high-concentration network has many more nodes than the low one, the average path lengths of these two networks are close. This phenomenon demonstrates that particles prefer to be organized in a compact aggregating way to construct a stable structure rather than to grow with a particular topological structure.

Summarizing the degree distribution, clustering coefficient and average path length, we see that these agglomeration networks are neither scale-free networks nor small-world networks. These features indicate that particles cannot be organized like social relations and or the internet; rather, they are restricted by space and coordination number. However, the relation between each particle is not as simple as our description. Hence, our data call for more complex and searching definitions to describe these unknown and unexplored connections in the future.

3.5. Degree correlations

The degree distribution completely determines the statistical properties of uncorrelated networks. However, as we shall see, a large number of real networks are correlated in the sense that the probability that a node of degree k is connected to another node of degree, say k', depends on k.

Degree correlation has been a subject of particular interest, because it can give rise to some interesting network structure effects. An interesting quantity related to degree correlations is the average degree of the nearest neighbors for vertices with degree k, denoted by $k_{\mathrm{nn}}(k)$ [41, 42], namely,

$$k_{nn} = \sum_{k'} k' P(k'|k). \tag{9}$$

When $k_{\mathrm{nn}}(k)$ increases with k, it means that vertices have a tendency to connect to vertices with a similar or larger degree. In this case the network is defined as assortative [43, 44]. In contrast, if $k_{\mathrm{nn}}(k)$ decreases with k, which implies that vertices of large degree are likely to have near neighbors with a small degree, then the network is said to be disassortative [45]. If correlations are absent, $k_{\mathrm{nn}}(k) = \mathrm{const}$.

As shown in figure 7 (with 5% error bars), $k_{\mathrm{nn}}(k)$ is approximately a linear function of k with a positive slope in the ranges of [2, 4] and [5, 8], which demonstrates that the networks are assortative.

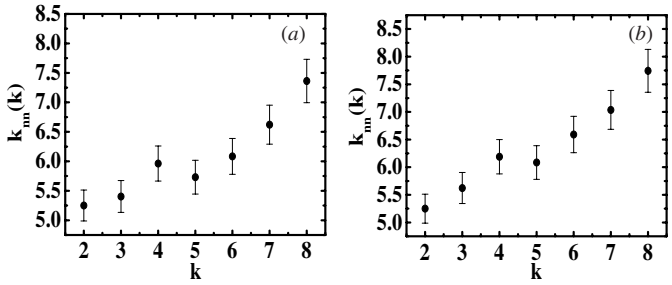

Figure 7. Assortative behavior is shown via the average nearest neighbor degree for (*a*) the low-concentration network and (*b*) the high-concentration network, respectively.

To confirm the assortativity, we describe degree correlations by a Pearson correlation coefficient r of the degrees at the ends of a link. It is defined as [43, 44, 46, 47]

$$r = \frac{\langle k\rangle\langle k^2 k_{nn}(k)\rangle - \langle k^2\rangle^2}{\langle k\rangle\langle k^3\rangle - \langle k^2\rangle^2}. \tag{10}$$

If the network is uncorrelated, the correlation coefficient vanishes. Disassortative networks have $r < 0$, while assortative graphs have a value of $r > 0$. We obtain $r = 0.45, 0.49$ for the low- and high-concentration networks, respectively, which testify to the assortativity of our two agglomeration networks. The assortativity implies that the nodes with a high degree prefer aggregating with their likes to attaching to ones of smaller degree for the sake of reducing the system energy as mentioned in section 3.1. Compared with disassortative networks, the exposed perimeter of assortative networks is smaller and the surface energy is also lower. Hence the assortativity in our networks is agrees with the results acquired in degree distribution.

3.6. Synchronizability

As mentioned in the preceding section, the definition of degree is the number of a pixel's neighbors. This definition is motivated by research on Raman optical activity enhancement [48]. When three bridging oxygen species act as the nearest neighbors of four bridging oxygen species, electronic coupling emerges between them. Hence we choose the nearest pixels as the neighbors connected with each pixel. In this section, we treat vertices as coupled oscillators on networks. At each node of a network is located an oscillator; a link connecting two nodes represents coupling between the two oscillators. A set of equations of motion governing the dynamics of the N coupled oscillators is

$$\dot{x}^i = F(x^i) + \sigma \sum_{j=1}^{N} G_{ij} W_{ij}, \tag{11}$$

where $\dot{x}^i = F(x^i)$ governs the dynamics of the individual oscillator, while σ is the coupling strength, where

$$F(x^i) = \sum_{j=1}^{k_i} \overrightarrow{F_{ij}}. \tag{12}$$

In this expression one has

$$F_{ij} = \frac{\partial E_{ij}}{\partial r_{ij}}. \tag{13}$$

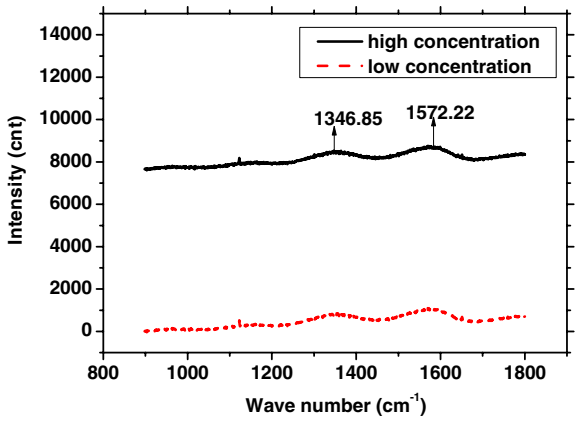

Figure 8. Raman spectra of two agglomerations.

Here, E_{ij} is total vibrational energy between node i and node j, r_{ij} stands for average bond length of interactional atoms between pixels i and j. Briefly, we only take the bond stretching energy shift E_k into consideration [49]:

$$E_{ij} = \sum_k E_k = \sum_k D_e\big\{1 - \exp\big[-a\big(b_k - b_{k_0}\big)\big]\big\}^2, \tag{14}$$

where D_e is the minimum of potential energy of atom pair k, $a = \omega\sqrt{\mu/2D_e}$ in which ω is the vibration frequency of the chemical bond in atom pair k. μ is the reduced mass, while $\omega = \sqrt{S/\mu}$ (S stands for the bond constant). In equation (10), b_{k_0} is the referenced bond length of an atom pair k (one atom of this atom pair belongs to pixel i and the other one belongs to pixel j) and b_k is the real bond length. k is the number of interactional atoms between pixel i and j:

$$W_{ij} = E_{ij}(\omega') - E_{ij}(\omega^0), \tag{15}$$

where ω' is the increased vibration frequency caused by laser energy absorbed and ω^0 is original vibration frequency, respectively. W_{ij} is total vibrational energy shift of interactional atoms between pixel i and j after laser activation. The $N \times N$ coupling matrix G is defined by $G_{ii} = k_i$ if the degree of node i is k_i, $G_{ij} = -1$ if nodes i and j are connected, and $G_{ij} = 0$ otherwise. The eigenratio γ (nonzero maximal eigenvalue to minimal eigenvalue) of the coupling matrix G quantifies the synchronizability of the network [50, 51]. That is to say, the smaller γ is, the better the synchronizability is, and vice versa. In this paper, we concentrate on how the network topology affects the eigenratio γ. We acquire $\gamma_{\text{low}} = 11.4456/0.0097 = 1180$ in an agglomeration of 358 pixels and $\gamma_{\text{high}} = 11.8682/0.0115 = 1032$ in an agglomeration of 896 pixels, that is to say, the agglomeration in the high-concentration solution have more oscillators but better synchronizability. Better synchronizability indicates that the agglomeration is more homogeneous as regards topology. In other words, the system at the high concentration is closer to a regular network.

In a word, the same indigenous materials formed under distinct conditions could turn to different agglomerations with different synchronizability. The agglomerations which have better synchronizability can absorb more photons at a certain wave number standing for a certain kind of oscillation. At the same time, people could find higher absorbing peak intensity. Hence, we conclude that difference of synchronizability is one of the common reasons for the physical enhancement of Raman spectra in the aggregating processes. During

the merging process, particles of agglomeration reform in a more compact way to reach a stable state, meanwhile, because of compact arranging [52], the synchronizability of these agglomerations becomes stronger and stronger. As a result, better synchronizability leads to higher absorbing intensity. For the sake of validating our conclusion, we choose two compact points with an approximately identical number of particles but different topology structures surrounding to test their Raman scattering intensity (see figure 8). These two nodes exist at the center of two agglomerations (one in low concentration and the other one in high concentration). It is obvious that the pixel in high concentration has higher intensity, while the one in low concentration absorbs less photons, which supports our conclusion.

4. Conclusion and discussion

Network science offers a different perspective on the topology of agglomerations. Our results indicate that agglomeration networks exhibit many interesting topological properties: a given pixel tends to have eight neighbors in two different agglomeration networks; low-concentration agglomerations have a larger clustering coefficient; the average path length of these two networks is close to each other; the networks are assortative in the domains; meanwhile the Pearson coefficient is positive. Self-similarity exists in the present agglomeration networks. The synchronizability of agglomerations gives us a new method to characterize material and explain mechanisms of intensity enhancement in Raman spectra, that is, the structure with better synchronizability could have higher intensity enhancement.

However, our networks are built based on the fact that a pixel stands for a node. Hence, we have shrunk a large number of atoms existing in one pixel and supposed that these nodes are closely arrayed in the pixel. This mapping indeed ignores some microcosmic information, but it represents the information on the micron scale as a whole. Furthermore, the holistic characters are just the key point of the Raman scattering intensity ignored by researchers. Further research should enable us to discuss interactions in agglomeration networks in greater detail.

Acknowledgments

We benefited from useful discussions with Shiming Cai and Jie Ren. We wish to thank Zhongzhi Zhang, Tao Zhou and WenXu Wang for their help with the manuscript. This research was supported by the National Basic Research Program of China under grant no 2007CB310806, the National Natural Science Foundation of China under grant nos 60496327, 60573183 and 90612007, and the Program for New Century Excellent Talents in the University of China (NCET-06-0376).

References

[1] Watts D J and Strogatz S H 1998 *Nature (London)* **393** 440
[2] Barabási A L and Albert R 1999 *Science* **286** 509
[3] Strogatz S H 2001 *Nature* **410** 268
[4] Albert R and Barabási A L 2002 *Rev. Mod. Phys.* **74** 47
[5] Dorogvtsev S N and Mendes J F F 2002 *Adv. Phys.* **51** 1079
[6] Newman M E J 2003 *SIAM Rev.* **45** 167
[7] Satorras R P and Vespignani A 2003 *Evolution and Structure of the Internet: A Statistical Physics Approach* (Cambridge: Cambridge University Press)
[8] Barabási A L, Ravasz E and Vicsek T 2001 *Phys.* A **299** 559
[9] Iguchi K and Yamada H 2005 *Phys. Rev.* E **71** 036144

[10] Alava M J and Dorogovtsev S N 2005 *Phys. Rev.* E **71** 036107
[11] Kim B J, Trusina A, Minnhagen P and Sneppen K 2000 *Eur. Phys. J.* B **13** 547
[12] Comellas F, Fertin G and Raspaud A 2004 *Phys. Rev.* E **69** 037104
[13] Jung S, Kim S and Kahng B 2002 *Phys. Rev.* E **65** 056101
[14] Ravasz E, Somera A L, Mongru D A, Oltvai Z N and Barabasi A L 2002 *Science* **297** 1551
[15] Ravasz E and Barabási A L 2003 *Phys. Rev.* E **67** 026112
[16] Zhang Z Z, Rong L L and Guo C H 2003 *Physica* A **363** 567
[17] Zhang Z Z, Rong L L and Zhou S G 2006 *Phys. Rev.* E **74** 046105
[18] Barrat A and Weigt M 2000 *Eur. Phys. J.* B **13** 547
[19] Lago-Fernández L F, Huerta R, Corbacho F and Siguenza J A 2000 *Phys. Rev. Lett.* **84** 2758
[20] Kim B J, Hong H, Holme P, Jeon G S, Minnhagen P and Choi M Y 2001 *Phys. Rev.* E **64** 056135
[21] Hong H, Choi M Y and Kim B J 2002 *Phys. Rev.* E **65** 026139
[22] Huberman B A and Adamic L 1999 *Nature* **401** 131
[23] Eckmann J P and Moses E 2002 *Proc. Natl Acad. Sci. USA* **99** 5825
[24] Menczer F 2002 *Proc. Natl Acad. Sci. USA* **99** 14014
[25] Hartwell L H, Hopfield J J, Leibler S and Murray A W 1999 *Nature* **402** 6761
[26] Concas G, Locci M F, Marchesi M, Pinna S and Turnu I 2006 *Europhys. Lett.* **76** 1221
[27] Sigman M and Cecchi G A 2002 *Proc. Natl Acad. Sci. USA* **99** 3
[28] Broder A, Kumar R, Maghoul F, Raghavan P, Rajagopalan S, Stata R, Tomkins A and Wiener J 2000 *Comput. Netw.* **33** 309
[29] Jeong H, Mason S P, Barabási A L and Oltvai Z N 2001 *Nature* **411** 41
[30] Barrat A, Barthélemy M, Satorras R P and Vespignani A 2004 *Proc. Natl Acad. Sci. USA* **101** 3747
[31] Jeong H, Tombor B, Albert R, Oltvai Z N and Barabási A L 2000 *Nature* **407** 651
[32] Newman M E J 2001 *Proc. Natl Acad. Sci. USA* **98** 404
[33] Liljeros F, Edling C R, Nunes Amaral L A, Stanley H E and Aberg Y 2001 *Nature* **411** 907
[34] Garlaschelli D, Caldarelli G and Pietronero L 2003 *Nature* **423** 165
[35] Mo Y, Morprke I and Wachter P 1984 *Solid State Commun.* **50** 829
[36] Johnson P B and Christy R W 1974 *Phy. Rev.* B **9** 5056
[37] Song C M, Havlin S and Makse H A 2005 *Nature* **433** 392
[38] Song C M, Havlin S and Makse H A 2006 *Nature Phys.* **2** 275
[39] Song C M, Gallos L K, Havlin S and Makse H A 2007 *J. Stat. Mech.* 03 P03006
[40] Fronczak A, Fronczak P and Holyst J A 2004 *Phys. Rev.* E **701** 056110
[41] Satorras R P, Vázquez A and Vespignani A 2001 *Phys. Rev. Lett.* **87** 258701
[42] Vázquez A, Pastor-Satorras R and Vespignani A 2002 *Phys. Rev.* E **65** 066130
[43] Newman M E J 2002 *Phys. Rev. Lett.* **89** 208701
[44] Newman M E J 2003 *Phys. Rev.* E **67** 026126
[45] Wang W X, Hu B, Wang B H and Yan G 2006 *Phys. Rev.* E **73** 016133
[46] Doye J P K and Massen C P 2005 *Phys. Rev.* E **71** 016128
[47] Ramasco J J, Dorogovtsev S N and Satorras R P 2004 *Phys. Rev.* E **70** 036106
[48] You J L, Jiang G C, Hou H Y, Chen H, Wu Y Q and Xu K D 2005 *J. Raman Spectrosc.* **36** 237
[49] Morse P M 1929 *Phys. Rev.* **34** 57
[50] Zhao M, Zhou T, Wang B H and Wang W X 2005 *Phys. Rev.* E **72** 057102
[51] Yin C Y, Wang W X, Chen G and Wang B H 2006 *Phys. Rev.* E **74** 047102
[52] Moskovits M, Tay L L, Yang J and Haslett T 2002 *Top. Appl. Phys.* **82** 215